Selective Collapse of Nonlinear Time Reversed Electromagnetic Waves

Scott Roman, Rahul Gogna, Steven M. Anlage
Gemstone Team TESLA, CNAM, Physics Department
University of Maryland
College Park, MD 20742-4111 USA
anlage@umd.edu

Abstract: **We envision a WPT process based on time-reversed propagation of electromagnetic (EM) waves in a complex scattering environment. This process has been well documented for targeting of either a single linear or nonlinear object. We numerically demonstrate selective targeting between two diodes simultaneously with different degrees of nonlinearity in a two-dimensional ray-chaotic billiard model. We demonstrate a 10.1:1 power delivery aspect ratio between the two diodes.**

Keywords—nonlinear time reversal; selective targeting, wireless power transfer

I. INTRODUCTION

The ability to focus waves at a specific point in space and time is desirable for many applications. Time-reversal (TR) is one such process that allows for this type of spatial and temporal focusing [1-2]. Acoustic TR, for instance, has been used to destroy kidney stones by focusing ultrasonic waves on them inside the body without harming the individual, greatly reducing the discomfort of performing lithotripsy [1]. Time-reversal of sound waves has also been used to locate cracks in walls, providing information about the failure modes of these structures [1, 3]. With electromagnetic waves, TR has been used to securely transfer information between two sources through an exclusive data link that eavesdroppers may not access [4]. Similarly, TR may be used to transfer power to different devices without sending power to the entire room, creating a unique, wireless, transmission channel. It is clear that improving the TR process may impact many fields and disciplines.

Performing linear TR in an enclosure requires 4 steps [1-2]. (1) Broadcast an initial interrogation pulse into the enclosure at location A. (2) As the pulse reverberates in the cavity, record a response signal, also called a sona, at another location B. (3) Flip the recorded sona waveform in time. (4) Broadcast the time-reversed sona at location B, creating a reconstruction of the initial signal back at location A. The temporal symmetry of the wave equation implies that the time-reversed sona in the last step will result in the time-reversed initial waveform reconstructing at location A (but nowhere else in the enclosure). In this sense, energy is only transferred to the location of interest (Location A) and nowhere else. By rapidly repeating the TR process, a wireless transmission channel can be created to transfer power between two specific locations in an enclosure. Because TR relies on the coherent superposition of many low-intensity channels to deliver large amounts of power to a specific location, it is an inherently safe process compared to other methods of WPT, such as microwave beaming or high power induction, that generate large E-fields locally[REF].

In this paper, we focus on the nonlinear time-reversal (NLTR) process [4-5]. NLTR is similar to linear TR except that it utilizes a passive nonlinear object, a device that outputs a signal at a different frequency than the input signal when it is interrogated, to establish a pair of locations that exchange power. We envision the nonlinear object being both a 'beacon' for TR *and* a mechanism to rectify the EM signal for use in power applications.

In NLTR we collect both a linear sona purely from the broadcast location and a nonlinear sona from the object of interest. NLTR works without any knowledge about the exact location of the nonlinear object, as the nonlinear sona is uniquely created based on the object's location in the cavity. By filtering out either the linear or nonlinear frequencies from the overall recorded sona, it has been shown that selective targeting of either the linear port (e. the initial emitter of the interrogation pulse) or the nonlinear port (the nonlinear object) may be realized [4]. In this paper, we use the pulse-inversion method of filtering to efficiently isolate the nonlinear signal [5-6]. This method extracts the nonlinear sona by summing the sonas from interrogation and inverted interrogation pulses sent into the cavity. Due to the nonlinear nature of the response, the linear portion and odd-harmonics (1*f*, 3*f*, 5*f*, etc.) (where *f* is the carrier frequency of the initial pulse) are cancelled and the even-harmonic nonlinear portion (2*f*, 4*f*, 6*f*, etc.) are doubled in amplitude. In our case the nonlinear sona is dominated by the 2*f* response.

For applications in wireless transmission of power, it is useful to broadcast power to multiple receiving devices at the same time. We have shown numerically that this process may be

978-1-4673-7986-1/16/$31.00 ©2016 IEEE

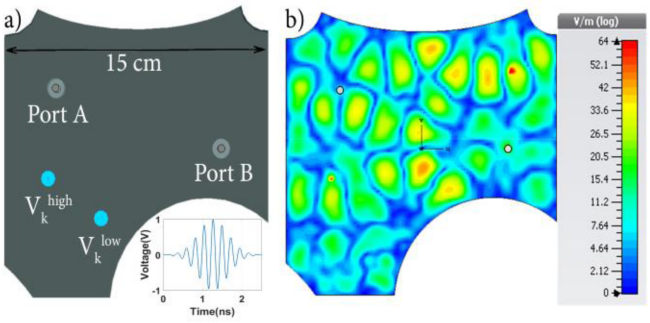

Figure 1: The cut-box simulation geometry used in CST. (a) shows the location of the 2 ports (A and B), 2 diodes (V_k^{high}, V_k^{low}), length scale, and the lower inset shows the initial interrogation pulse. (b) shows the electric field at a point in the simulation, illustrating the limited excited mode density.

performed with ease, providing the framework for a practical WPT system. Another useful aspect to this system is to selectively differentiate between different nonlinear objects, allowing a WPT system to choose which users will receive power to the exclusion of others. Imagine a scenario in which two cell phones are in a room and both need to be charged. We show that traditional NLTR allows for both phones to be charged simultaneously; however, we also demonstrate how one may charge one phone to the exclusion of the other.

II. Experimental

To establish a ray-chaotic setting for single-channel NLTR, we created a quasi-two-dimensional (2D) irregular cavity in CST. This cavity was a 15cm x 15cm x 0.76cm square box modified with various circular and elliptical segments removed from the walls as shown in Fig. 1. We used two Teflon-coated dipole antennas to emit and record signals [7]. Two diodes are placed inside the cavity, shown by the blue circles in Fig. 1. A 4.4 GHz center frequency pulse with a 1.0 GHz bandwidth was chosen to minimize the reflected power and applied to antenna A. This bandwidth was chosen due to the limited mode density present in our geometry, as TR requires many modes to be excited in the enclosure. In a larger cavity, such as a room in a building, the mode density would be much larger, allowing a smaller bandwidth to be used to excite the equivalent number of modes as shown in our simulation. The interrogation pulse used in our simulation is shown as an inset in Fig. 1 (a).

Given the frequency range and dimensions of the box, there are relatively few modes excited by the incident pulse (Fig. 1(b)), compared to the number of modes excited in a three-dimensional room, for example. This choice was imposed by our limited computational resources. As discussed later, we found that this limitation reduced but did not destroy our selective targeting signal fidelity.

In the simulation, we used a model diode to represent a passive nonlinear object. The nonlinear I-V curve causes the diode to have a significant harmonic current response when

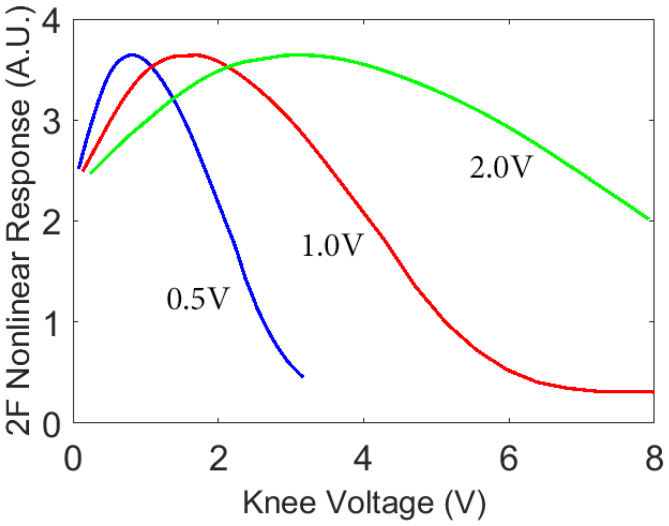

Figure 2: The nonlinear response of the model diode over different V_k values and different pulse amplitudes at a fixed 4.4 GHz center frequency with a 1.0 GHz bandwidth. A single value of V_k is found for each scenario that maximizes the nonlinear response. The blue, red, and green curves represent interrogation pulse amplitudes of 0.5V, 1.0V, and 2.0V respectively

excited above a specific voltage knee, V_k. CST defines the diode I-V characteristic as

$$I = I_o\left(e^{\frac{V}{V_k}a} - 1\right) \qquad (1)$$

Using $a = 1.3$, we defined V_k as the voltage needed to produce a current $I = 0.2\ I_0$, as this represented the approximate start of the nonlinear behavior.

Figure 2 shows the amplitude of response at the second harmonic frequency as a function of diode knee voltage for several different driving signal amplitudes at the fundamental frequency. The response was obtained by sweeping over many V_k values for different initial pulse amplitudes given the same geometry and process conditions as previously stated, where the pulse was emitted at Port A, the signal was recorded at port B, and the diode location was at the V_k^{low} diode position in Fig. 1(a). Fig. 2 shows that given a V_k value, we can choose a pulse amplitude to maximize nonlinear response. Fig. 2 also shows that for diodes with sufficiently large V_k, we observe a small nonlinear response, because the diode is not stimulated with voltages approaching V_k to produce a harmonic signal. Given this distribution, we may choose different amplitude interrogation pulses to target either a high-V_k or low-V_k diode.

III. Results and Discussion

In the simplest scenario, we may choose the same V_k for both diodes, causing both diodes to produce roughly the same strength harmonic response. After performing the full NLTR

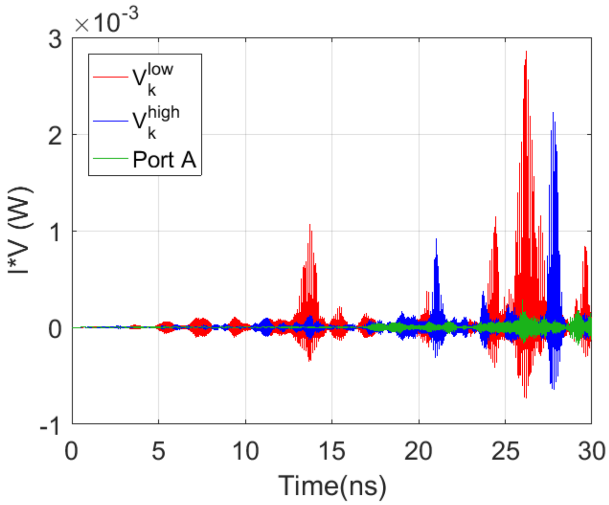

Figure 3: The instantaneous power monitored on the two diodes (shown in red and blue) as a function of time near the reconstruction time. Similar reconstructions occur on both diodes using NLTR when V_k is the same for both diodes. The non-target location near Port A (shown in green) receives a small amount of power relative to the two diodes.

process, this results in robust reconstructions at both diodes, as shown in Fig. 3. This establishes an important milestone in the use of NLTR as a WPT technology, as NLTR can transfer power to multiple locations of interest simultaneously. To determine the signal-to-noise ratio of the reconstruction, we measured the power in a diode in close proximity to Port A, shown in green in Fig 3, representing the power delivered at a non-target location in the cavity. This resulted in a signal-to-noise of 7.84:1 and 10.1:1 for the V_k^{low} and V_k^{high} diodes respectively. At this point, we may discuss how to selectively power one target to the exclusion of the other.

Here we show that exclusive targeting can take place in a system with multiple diodes present. We consider two diodes: one with V_k = 0.79 V (denoted V_k^{low}) and one with V_k = 6.60 V (denoted V_k^{high}). Given the large value of V_k^{high}, we expect to see no response in that diode while maintaining a reasonable nonlinear response in the V_k^{low} diode. We used a pulse with amplitude V = 1.0 V during the time forward step, emitted at Port A in Fig. 1(a). Using pulse-inversion, we extracted the nonlinear sona from the recorded signal at Port B, time-reversed the signal, and re-emitted it from Port B. Figure 4 shows the time-reversed reconstructions on both diodes. This results in a reconstruction almost exclusively on the V_k^{low} diode during the time-reversed step. To calculate the quality of the selective reconstruction, we determined the aspect ratio by comparing the maximum instantaneous power on both diodes. For this scenario, we calculate a power delivery aspect ratio of 10.1:1 for the V_k^{low} diode relative to the diode with V_k^{high}. This aspect ratio indicates that the V_k^{high} diode receives as much power as a non-target location, as shown previously in our simultaneous reconstruction experiment, where 7.81:1 and 10.1:1 signal-to-noise ratios were calculated for non-target locations.

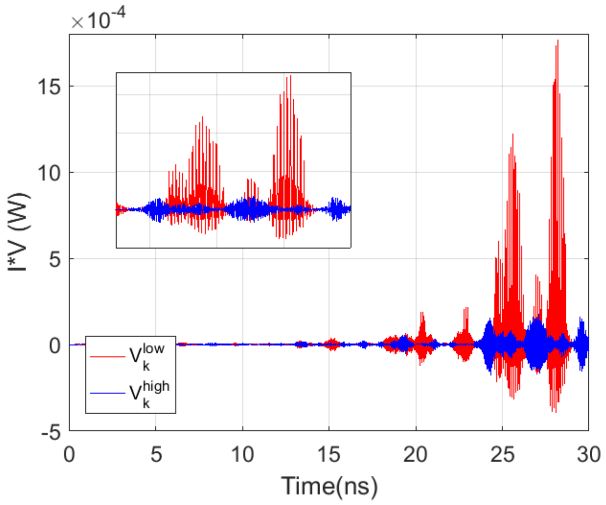

Figure 4: Time-reversed reconstructions on the two diodes while targeting V_k^{low}. Very little signal is seen on the V_k^{high} diode. The inset shows the details of the reconstructions between 23 and 30 ns.

IV. CONCLUSION

Our numerical results have illustrated a method to perform simultaneous and selective nonlinear time-reversal in the presence of multiple nonlinear objects in a cavity. In our simultaneous reconstruction simulation, we calculated the signal-to-noise ratio of the NLTR process to be 7.84:1 and 10.1:1 for the two diodes present. We also observed a delivered power aspect ratio of 10.1:1 for target power versus non-target power for selective targeting using NLTR. Further improvements are expected in this aspect ratio by increasing the enclosure mode density, sona collection time, number of channels in the NLTR mirror, and/or fine tuning the nonlinear object model. This ability to selectively target nonlinear objects in an enclosure can be used for wireless power applications by rectifying the reconstruction signals, allowing nonlinear time-reversal to transfer power to a DC load without knowledge of its location.

ACKNOWLEDGMENT

This work was supported by ONR through grant #N000141512134, the UMD Gemstone program, and CNAM. We would like to acknowledge all members of Gemstone Team TESLA for their feedback on results and data used in this paper.

REFERENCES

[1] Fink, Mathias. “Time-reversed Acoustics.” *Scientific American* 281, no. 5 (1999): 91–97.

[2] Blomgren, Peter, George Papanicolaou, and Hongkai Zhao. “Super-resolution in Time-reversal Acoustics.” *The Journal of the Acoustical Society of America* 111, no. 1 (2002): 230. doi:10.1121/1.1421342.

[3] Barbieri, E., and M. Meo. “Time Reversal DORT Method Applied to Nonlinear Elastic Wave Scattering.” *Wave Motion* 47, no. 7 (November 2010): 452–67. doi:10.1016/j.wavemoti.2010.01.004.

[4] Frazier, Matthew, Biniyam Taddese, Thomas Antonsen, and Steven M. Anlage. “Nonlinear Time Reversal in a Wave Chaotic System.” *Physical*

Review Letters 110, no. 6 (February 2013): 063902. doi:10.1103/PhysRevLett.110.063902.

[5] Simpson, David Hope, Chien Ting Chin, and Peter N. Burns. "Pulse Inversion Doppler: a New Method for Detecting Nonlinear Echoes from Microbubble Contrast Agents." *Ultrasonics, Ferroelectrics, and Frequency Control, IEEE Transactions On* 46, no. 2 (1999): 372–82.

[6] Hong, Sun K., Victor M. Mendez, Trystan Koch, Walter S. Wall, and Steven M. Anlage. "Nonlinear Electromagnetic Time Reversal in an Open Semireverberant System." *Physical Review Applied* 2, no. 4 (October 23, 2014): 044013. doi:10.1103/PhysRevApplied.2.044013.

[7] Hemmady, Sameer, Xing Zheng, Thomas M. Antonsen, Edward Ott, Steven M. Anlage, "Universal Properties of 2-Port Scattering, Impedance and Admittance Matrices of Wave Chaotic Systems," *Physical Review E* 74, no. 3 (2006): 036213. doi: 10.1103/PhysRevE.74.03621